# A Size-Efficient DFT Codebook Approach for DoA Estimation with Hybrid Arrays


Miguel Rivas-Costa and Carlos Mosquera

atlanTTic Research Center, Universidade de Vigo, Vigo, Spain
{mrivascosta,mosquera}@gts.uvigo.es



***Abstract*—Most existing direction-of-arrival (DoA) estimation techniques are tailored for fully digital (FD) antenna arrays. However, as modern MIMO systems scale to hundreds or thousands of antennas, FD architectures become increasingly impractical due to the prohibitive number of analog-to-digital converters (ADCs) required. Hybrid Analog-Digital (HAD) architectures offer a more hardware-efficient alternative, but conventional DoA estimation methods designed for FD arrays are not directly applicable in this setting. To overcome this challenge, we propose a novel method to reconstruct the covariance matrix of an equivalent FD array using measurements from a HAD architecture. This enables the application of classical subspace-based DoA estimation techniques with minimal adaptation. This work proposes a DFT-based codebook design which exploits the structure of Cauchy-like matrices for fast DoA estimation, making it particularly attractive for applications such as satellite-based or rapidly reconfigurable systems.**



***Index Terms*—Direction of arrival estimation, hybrid analog and digital arrays, covariance matrix reconstruction, array signal processing.**


## I. Introduction

Time-constrained beam alignment is of utmost importance in applications such as emerging non-terrestrial networks (NTN), with fast low earth orbit (LEO) satellites requiring accurate pointing under rapidly changing channel conditions [1]. Direction-of-arrival (DoA) estimation is the main signal processing tool available to determine the angle of incoming communication signals prior to their demodulation. It is also key for the tracking of interferers [2].

The vast majority of existing studies focus on fully digital (FD) architectures, where each antenna element is equipped with a dedicated analog-to-digital converter (ADC). Although FD arrays enable high-resolution processing, their implementation in modern multiple-input multiple-output (MIMO) systems is impractical due to the excessive cost and power consumption associated with a large number of ADCs [3]–[5].

To address these limitations, hybrid analog–digital (HAD) antenna arrays have been proposed as a cost-effective alternative, offering a trade-off between computational efficiency and hardware complexity. Various implementations have been explored, including Partially-Connected (PC), Fully-Connected (FC), and Switch-Based (SW) architectures [6]. In the specific case of PC and FC solutions, operation takes place in the beamspace, and convenient beamforming matrices, usually implemented by means of phase shifters, need to be designed. As a non exhaustive list, some representative works are [7]–[11]. More recently, deep neural networks (DNNs) have been explored as a data-driven alternative for DoA estimation, as demonstrated in [12], [13]. Furthermore, [14] presented an adaptive approach based on Discrete Fourier Transform (DFT) codebooks. Performance bounds have also been derived, see [6] and [15] for Cramér-Rao and Ziv-Zakai bounds, respectively.

Despite these advancements, many existing methods rely on restrictive assumptions, such as the presence of a single impinging signal or prior knowledge of signal and noise power. To address these limitations, an alternative approach based on covariance reconstruction was introduced in [16] for SW-based architectures. This method estimates the covariance matrix of the underlying FD array, enabling the use of classical DoA estimation techniques. This concept has been extended to HADs operating in the beamspace in [17] and subsequent refinements such as [18], [19] or [20] among others: a beam sweeping algorithm (BSA) is performed by analog beamforming to reconstruct the spatial covariance matrix for a number of incoming narrowband incoming signals non-necessarily constant. The number of predetermined angles is not properly determined in these works, and a sub-optimal diagonal loading parameter is needed for the reconstruction of the covariance matrix. This approach is refined in [21] for a single RF chain, with a reduction in complexity from $\mathcal{O}(N^3)$ to $\mathcal{O}(N \log N)$, based on an overcomplete DFT-based codebook with at least twice as many beams as antennas $N$.

The current paper addresses the DoA estimation of uncorrelated signals impinging on a FC-HAD for a very general signal model, not restricted to prior synchronized pilots or constant symbols. The focus is on fast acquisition, with a minimum size DFT-based codebook. The covariance matrix of the underlying digital array is associated with a *Cauchy-like* matrix, which is completed by means of the covariance matrices measured at the output of the successive beamformers, leading to an optimized number of angles to scan and estimation error improvement, particularly when the number of RF chains is


Work funded in part by MCIN/AEI/10.13039/501100011033/ FEDER "A way of making Europe" under project MAYTE (PID2022-136512OB-C22), and by Spanish Ministerio de Ciencia e Innovación (MICINN), project CASTRO (PID2021-122483OA-I00). Work supported in part by the Xunta de Galicia (Secretaría Xeral de Universidades) under a Predoctoral Scholarship (cofunded by the European Social Fund) ED481A 2022/407.

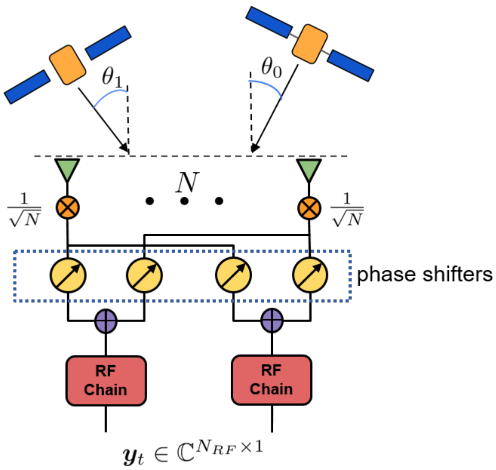


Fig. 1: Fully connected HAD architecture, with multiple phased subarrays. Two incoming signals.

high and the number of temporal snapshots is low.

## II. Signal Model

We consider a FC-HAD as depicted in Fig. 1 based on a Uniform Linear Array (ULA) with $N$ antennas and $N_{\text{RF}}$ RF chains, with separation between antennas equal to $d$. As a reasonable assumption for non-scattering environments, $L$ uncorrelated signals impinge on the array from directions $\{\theta_l\}$, $l = 0, \ldots, L-1$. In the narrowband case, the received signal after downconversion and sampling reads as[1]

$$\boldsymbol{y}_t = \boldsymbol{B}_t^H \boldsymbol{x}_t = \boldsymbol{B}_t^H \left(\boldsymbol{A}(\boldsymbol{\theta})\boldsymbol{s}_t + \boldsymbol{n}_t\right) \quad t = 0, \ldots, K-1, \quad (1)$$

for $K$ snapshots, where $\boldsymbol{B}_t \in \mathbb{C}^{N\times N_{\text{RF}}}$ is the beamforming matrix, possibly time-variant, with constant modulus weights given by $\boldsymbol{B}_t[u,v] = \frac{1}{\sqrt{N}} e^{j\phi_{uv}}$, with $\phi_{uv} \in [0, 2\pi)$. Note that $\boldsymbol{x}_t$ contains the baseband output samples of the FD array. The noise vector $\boldsymbol{n}_t \in \mathbb{C}^{N\times 1}$ follows a complex Gaussian distribution with zero mean and covariance $\sigma_n^2 \boldsymbol{I}_N$ and the transmitted signal vector $\boldsymbol{s}_t \in \mathbb{C}^{L\times 1}$ is also a complex Gaussian distributed with zero mean and covariance $\boldsymbol{R}_s = \text{diag}(\rho_0, \ldots, \rho_{L-1})$. The matrix $\boldsymbol{A}(\boldsymbol{\theta}) = (\boldsymbol{a}(\theta_0), \ldots, \boldsymbol{a}(\theta_{L-1})) \in \mathbb{C}^{N\times L}$ is formed by columns of the array manifold, which is supposed to be known under proper calibration:

$$\boldsymbol{a}(\theta_l) = \begin{pmatrix} 1 & e^{j\frac{2\pi d}{\lambda}\sin\theta_l} & \ldots & e^{j\frac{2\pi d}{\lambda}(N-1)\sin\theta_l} \end{pmatrix}^T. \quad (2)$$

After beamforming, the covariance matrix of the received signal $\boldsymbol{y}_t$ is given by $\mathbb{E}\{\boldsymbol{y}_t\boldsymbol{y}_t^H\} = \boldsymbol{B}_t^H \boldsymbol{R}_x \boldsymbol{B}_t$, where $\boldsymbol{R}_x \triangleq \boldsymbol{A}(\boldsymbol{\theta})\boldsymbol{R}_s\boldsymbol{A}^H(\boldsymbol{\theta}) + \sigma_n^2 \boldsymbol{I}_N$ represents the covariance of the corresponding FD array signal vector. The beamforming matrices $\boldsymbol{B}_t$ are taken from a codebook $\{\boldsymbol{B}_m\}$ to be designed of size $M \le K$.

[1]The Doppler effect induced by satellite motion has been evaluated and found to have a negligible impact on the results of this study; therefore, it is not considered in the analysis.

## III. 2D-DFT based reconstruction

Under the above signal model, the covariance matrix of the underlying FD array, $\boldsymbol{R}_x$, is Hermitian Toeplitz so, it can be fully characterized by its first column $\boldsymbol{r}$. Toeplitz matrices have been extensively used in signal processing due to their structural properties, which enable efficient solutions to linear systems [22], [23]. However, in general, the Toeplitz structure is lost after beamforming. As noted in [24], the two dimensional DFT (2D-DFT) of the Toeplitz matrix $\boldsymbol{R}_x$, expressed as $\boldsymbol{S} = \boldsymbol{F}^H \boldsymbol{R}_x \boldsymbol{F}$, has a *Cauchy-like* displacement structure. Specifically, when using the centered DFT matrix, defined as $\boldsymbol{F}[u,v] = \frac{1}{\sqrt{N}} e^{j2\pi/N(v-N/2)u}$, $u, v = 0, \ldots, N-1$, the entries of $\boldsymbol{S}$ satisfy

$$\boldsymbol{S}[u,v] = \begin{cases} \frac{2j}{N}\frac{\text{Im}\{S_u - S_v\}}{1-e^{j2\pi(v-u)/N}} & \text{if } u \neq v \\ 2\text{Re}\left\{S_u - \frac{1}{N}e^{-j2\pi/N(u-N/2)}S'_v\right\} & \text{if } u = v \end{cases} \quad (3)$$

where

$$S_u \triangleq \frac{\boldsymbol{r}[0]}{2} + \sum_{k=1}^{N-1} \boldsymbol{r}[k] e^{-j2\pi/N(u-N/2)k} \quad (4)$$

and

$$S'_u \triangleq \sum_{k=1}^{N-1} \boldsymbol{r}[k] k e^{-j2\pi/N(u-N/2)(k-1)}. \quad (5)$$

with $\boldsymbol{r}[n] = \boldsymbol{R}_x[n,0], n = 0, \ldots, N-1$. Eq. (3) reveals that the entries at the superdiagonal of $\boldsymbol{S}$, with $|u-v| = 1$, contain the required values to reconstruct the remaining off-diagonal entries. Note that specific values of the 2D-DFT $\boldsymbol{S}$ of $\boldsymbol{R}_x$ can be expressed as

$$\begin{aligned} \boldsymbol{S}[u,v] &= \frac{1}{N}\mathbb{E}\Big\{\sum_{p=0}^{N-1} \boldsymbol{x}_t[p] e^{-j\frac{2\pi}{N}(u-N/2)p} \sum_{q=0}^{N-1} \boldsymbol{x}_t^*[q] e^{j\frac{2\pi}{N}(v-N/2)q}\Big\} \\ &= \frac{1}{N}\sum_{p,q} \boldsymbol{r}[p-q] e^{-j\frac{2\pi}{N}(up-vq)} e^{j\pi(p-q)} \quad (6) \end{aligned}$$

with $\boldsymbol{r}[n] \triangleq \boldsymbol{r}^*[-n]$ for negative $n$, and where the summations within the expectation operator correspond to spatial frequency components that can be obtained with the proper DFT beam. Thus, if the codebook matrices $\{\boldsymbol{B}_m\}$ are composed of columns from $\boldsymbol{F}$, both the diagonal and superdiagonal entries can be obtained from the measurements $\boldsymbol{S}_m = \boldsymbol{B}_m^H \boldsymbol{R}_x \boldsymbol{B}_m$ for each $m = 0, \ldots, M-1$. For example, for $N_{\text{RF}} = 2$, $\boldsymbol{S}_0$ collects the values of the first $2 \times 2$ diagonal submatrix:

$$\boldsymbol{S} = \begin{pmatrix} \circ & \circ & \times & \cdots \\ \circ & \circ & \times & \cdots \\ \times & \times & \times & \cdots \\ \vdots & \vdots & \vdots & \ddots \end{pmatrix}. \quad (7)$$

See Fig. 2 for the corresponding codebook for $N = 4$. Note that $\boldsymbol{S}_m$ will be estimated by means of sample averages:

$$\hat{\boldsymbol{S}}_m = \frac{1}{Q}\sum_{t=mQ}^{mQ-1} \boldsymbol{B}_m^H \boldsymbol{x}(t)\boldsymbol{x}^H(t)\boldsymbol{B}_m \quad m = 0, \ldots, M-1. \quad (8)$$

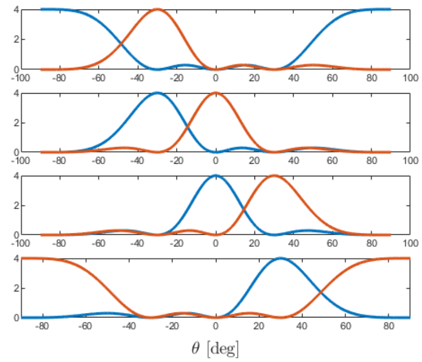


Fig. 2: Codebook radiation pattern $|\boldsymbol{B}_m^H \boldsymbol{a}(\theta)|^2, m = 0, 1, 2, 3,$ for $N = 4$ and $N_{\text{RF}} = 2$.

To simplify the notation, the symbol $\hat{\cdot}$ in $\hat{\boldsymbol{S}}_m$ will be omitted, although it is implicitly assumed that we operate with estimates.

Before introducing the codebook, we define a new indexing matrix $\boldsymbol{\mathcal{I}} \in \{0, \ldots, N-1\}^{M \times N_{\text{RF}}}$, which stores the indices of the columns $\{\boldsymbol{f}_n\}$ selected from $\boldsymbol{F}$. Using this matrix, the beamforming matrices in the codebook are constructed as

$$\boldsymbol{B}_m = \left( \boldsymbol{f}_{\boldsymbol{\mathcal{I}}[0,m]} \quad \cdots \quad \boldsymbol{f}_{\boldsymbol{\mathcal{I}}[N_{\text{RF}}-1,m]} \right). \tag{9}$$

The proposed codebook for covariance reconstruction is defined through the following indexing rule:

$$\boldsymbol{\mathcal{I}}[u, v] = \begin{cases} v & \text{if } \ u = 0 \\ (\boldsymbol{\mathcal{I}}[u-1, v] + N_{\text{RF}} - 1) \text{mod} N & \text{if } \ u \neq 0 \end{cases} \tag{10}$$

where the total number of beamforming matrices is

$$M = \begin{cases} \left\lceil \frac{N}{N_{\text{RF}}-1} \right\rceil & 1 < N_{\text{RF}} < N \\ 1 & N_{\text{RF}} = N. \end{cases} \tag{11}$$

We denote by $\lceil x \rceil$ the ceiling of $x$, i.e., the smallest integer greater than or equal to $x$. Note that for $N_{\text{RF}} = 1$, the results of [21] kick-in, and $M = 2N$.

This codebook ensures full coverage of the superdiagonal correlations by overlapping the last beam in each matrix $\boldsymbol{B}_m$ with the first beam in the subsequent matrix $\boldsymbol{B}_{m+1}$. Note that, strictly speaking, the reconstruction of $\boldsymbol{S}$ does not require the knowledge of $[\boldsymbol{S}]_{0,N-1}$. However, the absence of this spectral correlation creates a gap which degrades notably the performance when using practical estimates. This is why the last beamforming matrix includes both $\boldsymbol{f}_0$ and $\boldsymbol{f}_{N-1}$ to guarantee that the wrap-around correlation is also captured. Furthermore, since the correlation values are typically very small, they can be significantly affected in low signal-to-noise ratio (SNR) conditions. In consequence, a *least squares* estimate is applied to exploit the measurements of $\boldsymbol{S}$ beyond the superdiagonal, i.e., for $|u-v| > 1$. Note that, for $N_{\text{RF}} > 2$, correlation values between non-adjacent beams can be measured, contributing to reduce the error in $\boldsymbol{S}$ and, as a result, in $\boldsymbol{R}_x$. If $\tilde{\boldsymbol{s}}_m^i$ denotes the $i$th superior diagonal of the submatrix $\boldsymbol{S}_m$,

$$\tilde{\boldsymbol{s}}_m^i \triangleq (\boldsymbol{S}_m[0, i], \ldots, \boldsymbol{S}_m[N_{\text{RF}} - 1 - i, N_{\text{RF}} - 1])^T \tag{12}$$

with $i = 0, \ldots, N_{\text{RF}} - 1$, then we can write

$$\tilde{\boldsymbol{s}}_m^i = \tilde{\boldsymbol{A}}_m^i \tilde{\boldsymbol{r}} \tag{13}$$

where $\tilde{\boldsymbol{r}} \triangleq (\boldsymbol{r}[0], \boldsymbol{r}[1], \ldots, \boldsymbol{r}[N-1], \boldsymbol{r}^*[1], \ldots, \boldsymbol{r}^*[N-1])^T$ is the extended correlation vector, and $\tilde{\boldsymbol{A}}_m^i \in \mathbb{C}^{(N_{\text{RF}}-i) \times (2N-1)}$ follows from the relations of the *Cauchy-like* matrix $\boldsymbol{S}[u, v]$ in (3). In particular, it can be seen that the matrix entries read as

$$\tilde{\boldsymbol{A}}_m^0[u, v] = \tag{14}$$
$$\begin{cases} 1 & v = 0 \\ (1 - \frac{v}{N}) e^{j\pi v} e^{-j2\pi \boldsymbol{\mathcal{I}}[m,u] v/N} & v = 1, \ldots, N-1 \\ \tilde{\boldsymbol{A}}_m^{0,*}[u, v - N + 1] & v = N, \ldots, 2N-2. \end{cases}$$

and

$$\tilde{\boldsymbol{A}}_m^i[u, v] \overset{(i>0)}{=} \frac{1}{N(1 - e^{j2\pi i/N})}. \tag{15}$$
$$\cdot \begin{cases} 0 & v = 0 \\ e^{j\pi v}(1 - e^{-j2\pi i v/N}) e^{-j2\pi \boldsymbol{\mathcal{I}}[m,u] v/N} & v = 1, \ldots, N-1 \\ \tilde{\boldsymbol{A}}_m^{i,*}[u, v - N + 1] & v = N, \ldots, 2N-2. \end{cases}$$

Finally, to construct an overdetermined system of equations, all the entries from the upper diagonals of the $M$ projections $\{\boldsymbol{S}_m\}$ are collected in the vector $\tilde{\boldsymbol{s}} \triangleq (\tilde{\boldsymbol{s}}_0^{0,T}, \ldots, \tilde{\boldsymbol{s}}_0^{N_{\text{RF}}-1,T}, \ldots, \tilde{\boldsymbol{s}}_{M-1}^{0,T}, \ldots, \tilde{\boldsymbol{s}}_{M-1}^{N_{\text{RF}}-1,T})^T$, along with the corresponding coefficient matrices $\tilde{\boldsymbol{A}} \triangleq (\tilde{\boldsymbol{A}}_0^{0,T}, \ldots, \tilde{\boldsymbol{A}}_0^{N_{\text{RF}}-1,T}, \ldots, \tilde{\boldsymbol{A}}_{M-1}^{0,T}, \ldots, \tilde{\boldsymbol{A}}_{M-1}^{N_{\text{RF}}-1,T})^T$. With this, we minimize $\|\tilde{\boldsymbol{s}} - \tilde{\boldsymbol{A}}\tilde{\boldsymbol{r}}\|^2$ by means of the pseudoinverse:

$$\tilde{\boldsymbol{r}} = (\tilde{\boldsymbol{A}}^H \tilde{\boldsymbol{A}})^{-1} \tilde{\boldsymbol{A}}^H \tilde{\boldsymbol{s}}. \tag{16}$$

### A. *On the number of measurements*

A critical aspect in DoA estimation is the ability to localize targets as quickly as possible. To achieve this, it is essential to estimate the DoAs using the smallest possible number of snapshots. When the transmitted signal is constant, it is well-known that an exact reconstruction—equivalent to what would be obtained with a fully digital array—can be achieved with just $K = \left\lceil \frac{N}{N_{\text{RF}}} \right\rceil$ snapshots [25].

However, when the transmitted signal $\boldsymbol{s}(t)$ varies over time, such a tight bound cannot be guaranteed. The randomness in $\boldsymbol{s}(t)$ increases the variability of the projections $\{\boldsymbol{S}_m\}$, which in turn requires a larger number of snapshots to accurately estimate them. Despite this, minimizing the number of beamforming matrices in the codebook—denoted by $M$—remains highly desirable. This allows the total number of snapshots $K$ to be distributed more effectively, increasing the number of averages used per projection $\boldsymbol{S}_m$, and improving the estimation accuracy.

It has been shown recently in [26] that analog arrays, measuring the power at the output of single RF port, require to explore at least $M = 2N$ beams for perfect covariance reconstruction. Naturally, when multiple RF chains are available, the size of the codebook can be reduced proportionally to $M = \left\lceil \frac{2N}{N_{\text{RF}}} \right\rceil$. The results in this paper show that the size of this codebook can be further reduced by exploiting the correlation across beams, see Eq. (11), even by 50%, as Fig. 3 illustrates.

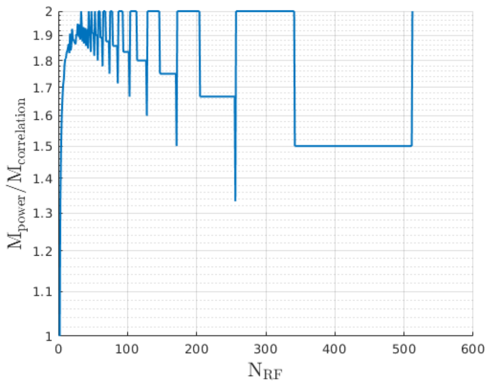


Fig. 3: Reduction factor of the codebook size when correlation across beams is exploited. $N = 512$.

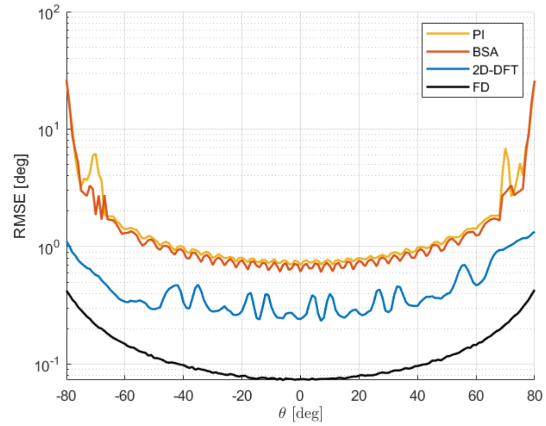


Fig. 4: RMSE as function of the DoA. $N = 16$, $N_{\text{RF}} = 4$, $K = 96$, $L = 1$, SNR $= 0$ dB.

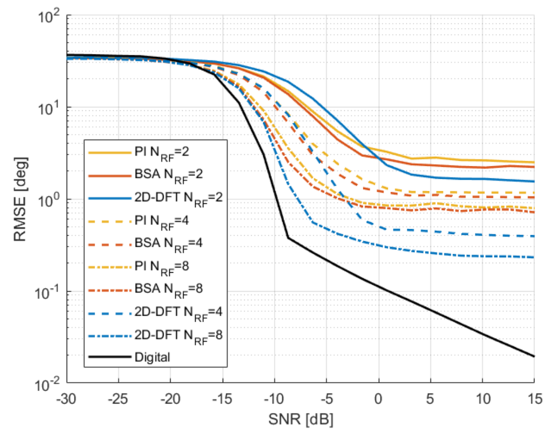


Fig. 5: RMSE as function of the SNR. $N = 16$, $N_{\text{RF}} = \{2, 4, 8\}$, $K = 96$, $L = 3$.

## IV. Simulations

For simulation purposes, we consider a ULA of $N = 16$ antennas, with inter-element spacing $d = \frac{\lambda}{2}$, receiving several narrowband signals. For simplicity, the signal power is assumed to be the same for all signals, $\sigma_s^2$, and the noise variance is normalized to one, so the signal-to-noise ratio (SNR) is directly SNR $\triangleq 10\log_{10}\sigma_s^2$. The covariance matrix $\boldsymbol{R}_x$ is estimated, and DoAs are computed with Root-MUSIC [27]. The reconstruction of the Cauchy-like two-dimensional DFT of the covariance matrix (2D-DFT) is compared with the Beam Sweeping Algorithm (BSA) [28] and the Phase Independent (PI) scheme [26]. In the former, the number of beams is $N$, and $2N$ in the two latter. For benchmarking purposes, the fully digital (FD) array performance is also displayed. The performance metric is the Root Mean Squared Error (RMSE):

$$\text{RMSE} \triangleq \sqrt{\frac{1}{L \cdot \text{MC}} \sum_{i=0}^{\text{MC}-1} \sum_{l=0}^{L-1} (\theta_{i,l} - \hat{\theta}_{i,l})^2} \tag{17}$$

with $L$ the number of signals, MC the number of Montecarlo realizations, and $\{\theta_{i,l}, \hat{\theta}_{i,l}\}$ the true and estimated angles of arrival, respectively.

The first experiment examines the impact of the incoming angle on the RMSE. The simulation is carried out for $N_{\text{RF}} = 4$ RF chains, $K = 96$ snapshots, and MC $= 10^4$ Monte Carlo realizations. A single signal with SNR $= 0$ dB is considered. As expected, Fig. 4 showcases a jagged error in the beam-based schemes operating with the HAD, due to the spatial non-uniformity of the beam patterns. The exploitation of the correlation across beams gives an important edge to the 2D-DFT method, more noticeable for a higher number of RF chains, as discussed next.

The analysis of the RMSE in scenarios with multiple incoming signals is also of interest. Fig. 5 illustrates the performance for $L = 3$ signals, whose DoAs are randomly selected from a grid with $10°$ spacing, within a $120°$ field of view spanning the range $(-60°, 60°)$. The number of RF chains is chosen from the set $\{2, 4, 8\}$. To account for the increased randomness in this scenario, the number of Monte Carlo realizations is set to MC $= 10^5$. Except for low SNR and $N_{\text{RF}} = 2$, 2D-DFT outperforms previous methods, with improvement growing with the number of RF chains. Note that in all cases there is an error floor due to the covariance matrix approximation error, which decreases with the sequence length, as seen next.

The parameters of the array in the third experiment remain the same as in the previous simulation: $N = 16$, $N_{\text{RF}} \in \{2, 4, 8\}$, and $L = 3$ signals impinging on the array with directions randomly drawn from $\theta_l \sim \mathcal{U}(-60°, 60°)$. In this scenario, the signal-to-noise ratio is set to SNR $= 0$ dB. Figure 6 presents the results of this experiment, which are consistent with the observations from the previous simulation. In particular, an increase in the number of snapshots contributes to decrease the saturation floor of the error.

## V. Conclusions

An accurate and fast direction-of-arrival (DoA) estimation method for hybrid arrays has been presented, oriented to critical steering applications such as satellite beam alignment,

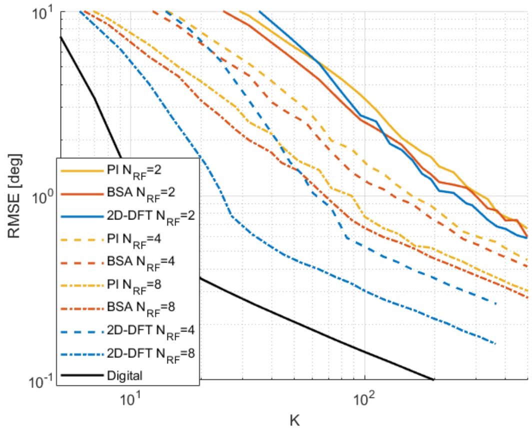


Fig. 6: RMSE as function of the number of snapshots. $N = 16$, $N_{\text{RF}} = \{2, 4, 8\}$, $L = 3$, SNR = 0 dB.

with rapidly changing channel conditions due to high mobility. Without imposing artificially restrictive signal models, the minimum number of beams required for covariance matrix reconstruction has been established. This enables a reduction in the estimation error for a given number of snapshots or, equivalently, a decrease in the acquisition time needed to achieve a target accuracy.

Future work will focus on reducing the computational complexity and extending the proposed approach to two-dimensional array geometries, representing a natural progression toward practical deployments.

## References


[1] G. Yılmaz, U. Gustavsson, and H. Joudeh, "Active Beam Training with Hierarchical Codebooks in Two-Dimensional Phased Arrays," in *25th IEEE International Workshop on Signal Processing Advances in Wireless Communications*, 2024.

[2] J. Yao, C. Zhao, J. Bai, Y. Ren, Y. Wang, and J. Miao, "Satellite Interference Source Direction of Arrival (DOA) Estimation Based on Frequency Domain Covariance Matrix Reconstruction," *Sensors*, vol. 23, no. 17, p. 7575, 2023.

[3] S. Han, C.-l. I, Z. Xu, and C. Rowell, "Large-scale antenna systems with hybrid analog and digital beamforming for millimeter wave 5G," *IEEE Communications Magazine*, vol. 53, no. 1, pp. 186–194, 2015.

[4] F. Rusek, D. Persson, B. K. Lau, E. G. Larsson, T. L. Marzetta, O. Edfors, and F. Tufvesson, "Scaling Up MIMO: Opportunities and Challenges with Very Large Arrays," *IEEE Signal Processing Magazine*, vol. 30, no. 1, pp. 40–60, 2013.

[5] A. L. Swindlehurst, E. Ayanoglu, P. Heydari, and F. Capolino, "Millimeter-wave massive MIMO: the next wireless revolution?," *IEEE Communications Magazine*, vol. 52, no. 9, pp. 56–62, 2014.

[6] R. Zhang, B. Shim, and W. Wu, "Direction-of-Arrival Estimation for Large Antenna Arrays With Hybrid Analog and Digital Architectures," *IEEE Transactions on Signal Processing*, vol. 70, pp. 72–88, 2022.

[7] R. Zhang, B. Shim, and W. Wu, "Direction-of-Arrival Estimation for Large Antenna Arrays With Hybrid Analog and Digital Architectures," *IEEE Transactions on Signal Processing*, vol. 70, pp. 72–88, 2022.

[8] F. Shu, Y. Qin, T. Liu, L. Gui, Y. Zhang, J. Li, and Z. Han, "Low-Complexity and High-Resolution DOA Estimation for Hybrid Analog and Digital Massive MIMO Receive Array," *IEEE Transactions on Communications*, vol. 66, no. 6, pp. 2487–2501, 2018.

[9] B. Shi, Q. Zhang, R. Dong, Q. Jie, S. Yan, F. Shu, and J. Wang, "DOA Estimation for Hybrid Massive MIMO Systems Using Mixed-ADCs: Performance Loss and Energy Efficiency," *IEEE Open Journal of the Communications Society*, vol. 4, pp. 1383–1395, 2023.

[10] J. A. Zhang, W. Ni, P. Cheng, and Y. Lu, "Angle-of-arrival estimation using different phase shifts across subarrays in localized hybrid arrays," *IEEE Communications Letters*, vol. 20, no. 11, pp. 2205–2208, 2016.

[11] C. Qin, J. A. Zhang, X. Huang, K. Wu, and Y. J. Guo, "Fast Angle-of-Arrival Estimation via Virtual Subarrays in Analog Antenna Array," *IEEE Transactions on Wireless Communications*, vol. 19, no. 10, pp. 6425–6439, 2020.

[12] F. Shu, Y. Chen, X. Zhan, W. Cai, M. Huang, Q. Jie, Y. Li, B. Shi, J. Wang, and X. You, "Machine-learning-aided Massive Hybrid Analog and Digital MIMO DOA Estimation for Future Wireless Networks," 2023.

[13] D. Hu, Y. Zhang, L. He, and J. Wu, "Low-Complexity Deep-Learning-Based DOA Estimation for Hybrid Massive MIMO Systems With Uniform Circular Arrays," *IEEE Wireless Communications Letters*, vol. 9, no. 1, pp. 83–86, 2020.

[14] A. Abdelbadie, M. Mostafa, S. Bameri, R. H. Gohary, and D. Thomas, "DoA Estimation for Hybrid Receivers: Full Spatial Coverage and Successive Refinement," *IEEE Transactions on Signal Processing*, vol. 72, pp. 4730–4744, 2024.

[15] M. Rivas-Costa and C. Mosquera, "Direction of Arrival Estimation with Hybrid Digital Analog Arrays: Algorithms and Ziv-Zakai Lower Bound," in *2023 57th Asilomar Conference on Signals, Systems, and Computers*, pp. 1329–1333, IEEE, 2023.

[16] D. D. Ariananda and G. Leus, "Direction of arrival estimation of correlated signals using a dynamic linear array," in *2012 Conference Record of the Forty Sixth Asilomar Conference on Signals, Systems and Computers (ASILOMAR)*, pp. 2028–2035, 2012.

[17] S. Li, Y. Liu, L. You, W. Wang, H. Duan, and X. Li, "Covariance matrix reconstruction for DOA estimation in hybrid massive MIMO systems," *IEEE Wireless Communications Letters*, vol. 9, no. 8, pp. 1196–1200, 2020.

[18] Y. Liu, Y. Yan, L. You, W. Wang, and H. Duan, "Spatial Covariance Matrix Reconstruction for DOA Estimation in Hybrid Massive MIMO Systems With Multiple Radio Frequency Chains," *IEEE Transactions on Vehicular Technology*, vol. 70, no. 11, pp. 12185–12190, 2021.

[19] Y. Yan, Y. Liu, and H. Duan, "Adaptive Reconstruction for Spatial Covariance Matrix in Hybrid Massive MIMO Systems," *IEEE Access*, vol. 9, pp. 145060–145065, 2021.

[20] Y. Zhou, B. Dang, Y. Li, and G. Liu, "An Efficient Spatial Covariance Matrix Reconstruction Algorithm in the Hybrid Analog-Digital Structure," *IEEE Transactions on Vehicular Technology*, vol. 71, no. 7, pp. 7930–7935, 2022.

[21] O. Shmonin, V. Kuptsov, S. Trushkov, K. Ponur, G. Serebryakov, H. Wang, and J. Zhang, "Phase-Independent Beamspace MUSIC Algorithm for a Single Port Phased Antenna Array," in *2023 31st Telecommunications Forum (TELFOR)*, pp. 1–4, 2023.

[22] S. Chandrasekaran, M. Gu, X. Sun, J. Xia, and J. Zhu, "A Superfast Algorithm for Toeplitz Systems of Linear Equations," *SIAM Journal on Matrix Analysis and Applications*, vol. 29, no. 4, pp. 1247–1266, 2008.

[23] R. W. Heath, N. González-Prelcic, S. Rangan, W. Roh, and A. M. Sayeed, "An Overview of Signal Processing Techniques for Millimeter Wave MIMO Systems," *IEEE Journal of Selected Topics in Signal Processing*, vol. 10, no. 3, pp. 436–453, 2016.

[24] G. Heinig and A. Bojanczyk, "Transformation techniques for Toeplitz and Toeplitz-plus-Hankel matrices. I. Transformations," *Linear Algebra and its Applications*, vol. 254, no. 1-3, pp. 193–226, 1997.

[25] M. Trigka, C. Mavrokefalidis, and K. Berberidis, "Full snapshot reconstruction in hybrid architecture antenna arrays," *EURASIP Journal on Wireless Communications and Networking*, vol. 2020, pp. 1–22, 2020.

[26] O. Shmonin, V. Kuptsov, S. Trushkov, K. Ponur, G. Serebryakov, H. Wang, and J. Zhang, "Phase-Independent Beamspace MUSIC Algorithm for a Single Port Phased Antenna Array," in *2023 31st Telecommunications Forum (TELFOR)*, pp. 1–4, 2023.

[27] H. L. V. Trees, *Optimum Array Processing: Detection, Estimation and Modulation Theory, Part IV*. John Wiley & Sons, 2002.

[28] Z. Fu, Y. Liu, and Y. Yan, "Fast Reconstruction and Iterative Updating of Spatial Covariance Matrix for DOA Estimation in Hybrid Massive MIMO," *IEEE Access*, vol. 8, pp. 213206–213214, 2020.